COMBINED STEADY-STATE AND DYNAMIC HEAT EXCHANGER EXPERIMENT

WILLIAM LUYBEN, KEMAL TUZLA, AND PAUL BADER
Lehigh University • Bethlehem, PA 18015

Dow Chemical Co. provided a pilot-scale heat-transfer experiment to the Department of Chemical Engineering at Lehigh University about 20 years ago. This experiment has been an important fixture in our unit operations laboratory since that time. Only steady-state experiments and analysis were performed for most of this period. The equipment has been modified recently to permit experiments involving dynamic control studies.

The steady-state aspects of the experiment involve taking flowrate, temperature, and pressure data so that energy balances around each heat exchanger can be calculated. Flowrates are measured by orifice plates and differential pressure transmitters, but are also checked by the old reliable "bucket and stop watch" method. There are duplicate temperature measurements at some locations (thermocouple and dial thermometer) to give the students an understanding of the inherent discrepancy between different devices. Overall heat-transfer coefficients are calculated, and Wilson plots are made to determine inside film coefficients at different process-water flowrates. Experimental results are compared with the predictions of applicable correlations in the literature.

The dynamic aspects of the experiment involve dynamic tests (step and relay-feedback) and closedloop control of two process temperatures (process outlet temperature from the heater and process outlet temperature from the cooler) by manipulation of steam and cooling water flowrates, respectively. Computer simulations of the system are developed, both steady state and dynamic, and results are compared with experimental data.

William Luyben *is a professor of chemical engineering at Lehigh University. He received his B.S. from Penn State and his Ph.D. from the University of Delaware. He teaches Unit Operations Laboratory, Process Control, and Plant Design courses. His research interests include process design and control, distillation, and energy processes.*

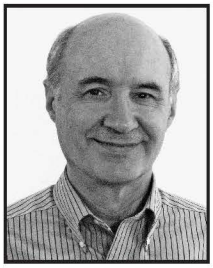

Kemal Tuzla *is a professor of practice and associate chair in the Department of Chemical Engineering at Lehigh University. He received his B.S. and Ph.D. from the Technical University of Istanbul. He teaches Unit Operations Laboratory, Fluid Mechanics, and Heat Transfer courses. His research interests include heat transfer in two-phase flows and thermal energy storage.*

Paul Bader *is senior electronics technician in the Department of Chemical Engineering at Lehigh University. His special interest is the unit operations experiments. In the present work he designed and implemented the control loop for the heat exchanger experiment.*

PROCESS DESCRIPTION

Figure 1 shows the flowsheet of the process. Figure 2 gives a picture of the apparatus. Water from a tank (0.71 m ID, 1.2 m height) is pumped by a 15 hp centrifugal pump to the heater, which is a two-pass tube-in-shell heat exchanger with 0.542 m^2 inside heat-transfer surface. Table 1 gives details of the heat exchanger equipment. Material of construction is stainless steel.

Saturated steam at 3.36 bar from a steam header passes through a pneumatically operated control valve (CV = 25, air-to-open, equal-percentage trim) into the shell side of the heater. Steam pressure in the shell side of the heater is about 1.8 bars under typical steady-state conditions, which corresponds to a saturation temperature of 117 °C. Condensate leaves the heater as saturated liquid through a steam trap. It goes to a three-way valve that permits bucketing the condensate flowrate or discharging into a drain.

The process water then flows into the cooler, which is a 4-pass tube-in-shell heat exchanger with 2.957 m^2 of heat-transfer area. Cooling water from a supply header at 3.7 bars flows into the shell side of the cooler. The temperature of the cooling water supply is generally around 7 °C. After flowing through the cooler, the cooling water passes through a pneumatically operated control valve (CV = 9, air-to-close, equal-percentage trim) and goes to a three-way valve that permits bucketing the cooling-water flowrate or discharging into a drain. The process water then flows through a control valve (CV = 12, air- to-close, equal-percentage trim) and back into the feed tank. Temperatures are measured at numerous locations and are shown on the flowsheet given in Figure 1. The three control valves are pneumatic, so the electronic signals (4 to 20 mA) from the computer control system are fed to three I/P transducers.

WILSON PLOT METHOD

In a tube-in-shell heat exchanger, the overall heat-transfer coefficient U is defined as follows.

$$\frac{1}{UA}=\frac{1}{U_0A_0}=\frac{1}{U_iA_i}=\frac{1}{h_iA_i}+R_{f0}+\frac{\ln\left(\frac{D_0}{D_i}\right)}{2\pi kL}+R_{fi}+\frac{1}{h_0A_0} \quad (1)$$

where A_i and A_0 represent inside and outside heat-transfer surface areas of a single tube, h_i and h_0 are inside and outside film coefficients, R_{fi} and R_{f0} are inside and outside fouling resistances, D_i and D_0 are inside and outside diameters of the tubes, k is the thermal conductivity of the metal tube wall and L is the tube length. Using the inside surface area of the tubes as the basis,

$$\frac{1}{U_i}=\frac{1}{h_i}+A_i\left[R_{fi}+\frac{\ln\left(\frac{D_0}{D_i}\right)}{2\pi kL}+R_{fo}\right]+\frac{1}{h_0\frac{A_0}{A_i}} \quad (2)$$

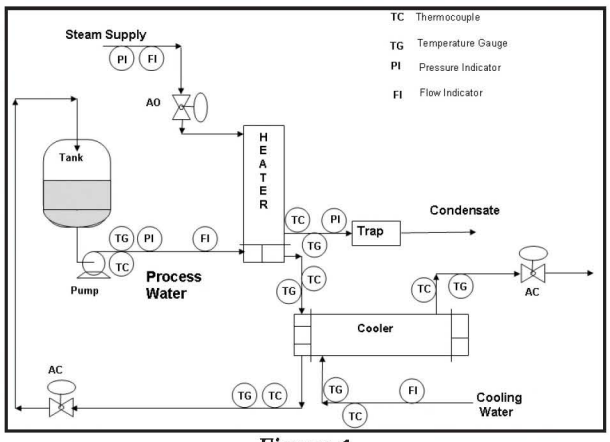

Figure 1.

Figure 2.

Wilson[1] suggested that experiments can be run to find a relationship between the overall heat-transfer coefficient (U_i) and the film coefficient inside the tube (h_i). In these experiments, the wall resistance, inside and outside fouling and outside film coefficient must be held constant, see also Hewitt, *et al.*[2]

If we call the sum of the second and the third terms on the right hand side of Eq. (2) constant "A"

$$\frac{1}{U_i}=\frac{1}{h_i}+A \quad (3)$$

TABLE 1
Heat Exchanger Parameters

	Heater	Cooler
Number passes	2	4
Heat-transfer area (inside) (m^2)	0.542	2.957
Number of tubes	108	104
Tube ID (m)	0.00475	0.00775
Wall thickness (m)	0.0008	0.00089
Tube Length (m)	0.337	1.17
Shell ID (m)	0.105	0.206

$$\text{Where, } A = A_i\left[R_{fi} + \frac{\ln\left(\frac{D_0}{D_i}\right)}{2\pi kL} + R_{fo}\right] + \frac{1}{h_o\frac{A_0}{A_i}} \qquad (3a)$$

For fluid flowing inside tubes, h_i can be expressed as

$$Nu = \frac{h_i D_i}{k} = C\,Re^m\,Pr^n \qquad (4)$$

where C, m, and n are constants that depend on the fluid and flow conditions. Thus, h_i can be expressed as,

$$h_i = \frac{k}{D_i}\cdot C\left(\frac{\rho D}{\mu}\right)^m\cdot(v)^m\cdot Pr^n \qquad (5)$$

Or, if we keep the properties of the fluid constant,

$$h_i = \frac{1}{B}\cdot v^m$$

$$\text{where } \frac{1}{B} = C\cdot\frac{k}{D_i}\left(\frac{\rho D}{\mu}\right)^m\cdot Pr^n \qquad (6)$$

Introducing this into Eq. (3) gives

$$\frac{1}{U_i} = B\frac{1}{v^m} + A \qquad (7)$$

Experiments can be carried out by keeping the operating parameters in "A" and "B" constant while varying velocity of the flow inside the tube. Measurements of overall heat-transfer coefficients then provide the values of the constants "A" and "B" if the parameter m is known. The data presented here were obtained from experiments that are carried out in the turbulent regime where m = 0.8. The constant "C" in Eq. (4) can also be calculated.

To keep the operating heat-transfer parameters constant on the shell sides of both heat exchangers, the following conditions are established:

- *The temperature driving force ($T_S - T_{Wall}$) on the shell side of the heater is kept constant in order to have similar film coefficients during condensation of the steam.*
- *Cooling water flowrate on the shell side of the cooler is kept at its maximum value in order to have a fixed and a high film coefficient.*

With the above conditions, the Wilson plot method can be applied to the data to extract tube-side film coefficients from the measured overall heat-transfer coefficients over a range of process water flowrates.

INSTRUMENTATION CALIBRATION AND DATA RECONCILIATION

There are two different temperature sensors at every location where temperature is measured (thermocouples and gauges). There are up to ±2 °C differences between sensor outputs. Therefore all sensors are calibrated based on a reference temperature measurement device.

Flowrates are sensed using orifice plates and pressure differences and are recorded using a computer-based data acquisition system. Calibrations are carried out using the bucket and stopwatch method.

Even with these calibrations, the inaccuracies in the experimental data do not give perfect energy balances, so the students learn that some engineering judgment is required to reconcile the data. Temperature data is adjusted so that the calculated energy balances on both sides of both exchangers match perfectly.

EXPERIMENTAL DATA AND SAMPLE CALCULATIONS

Experimental measurements consist of recording of the following data:

- *Process water inlet temperature to heater—$T_{PWH,in}$*
- *Process water outlet temperature from heater—$T_{PWH,out}$*
- *Process water outlet temperature from cooler—$T_{PWC,out}$*
- *Saturation temperature of the condensing steam on the*

TABLE 2
Experimental Data

Description of Parameters	TP1	TP2	TP3	TP4	TP5	TP6
PW Inlet Temp. to Heater (°C)	23.25	36.16	34.00	34.00	34.59	35.67
PW Outlet Temp. From Heater (°C)	61.79	72.63	68.24	67.68	66.03	64.93
PW Outlet Temp. from Cooler (°C)	22.40	32.51	33.26	34.71	34.71	36.91
Condensate temperature (°C)	118.23	120.55	118.89	121.67	120.55	120.55
CW Inlet Temp. to Cooler (°C)	6.79	7.8	7.22	6.7	7.22	7.22
CW Outlet Temp. from Cooler (°C)	21.95	31.67	31.11	33.33	33.33	34.44
PW Flow Rate (kg/s)	0.241	0.667	0.8275	0.953	1.0435	1.099
Steam Flow Rate (kg/s)	0.0207	0.0473	0.0482	0.0491	0.0498	0.0514
CW Flow Rate (kg/s)	1.1	1.1	1.1	1.1	1.1	1.1

shell side of the heater—T_S

- *Flow rate of the process water*—F_{PW}
- *Flow rate of the steam*—F_S
- *Flow rate of the cooling water*—F_{CW}

Table 2 (previous page) gives raw experimental data for six runs with varying process-water flowrates.

To illustrate the calculations and data reconciliation, we take Run TP3 with a process water flowrate of 0.8275 kg/s.

A. Energy Balances

Under steady-state conditions, if there were no heat losses in the system, the heat gained by the process water in the heater would equal the heat lost by the process water in the cooler. Likewise, the heat lost by the steam would be equal to the heat gained by the process water, and the heat gained by the cooling water would be equal to the heat lost by the process water. Therefore, all four of the heat-transfer rates should be equal.

1. Heater:

The heat-transfer rate is calculated on the process-water side of the heater using Eq. (8) from the measurements of the process-water flowrate and its inlet and outlet temperatures.

$$Q_{PWH} = F_{PW} c_p \left(T_{PWH,out} - T_{PWH,in}\right) \tag{8}$$

$$Q_{PWH} = 0.8275\ \text{(kg/s)}\ 4.193\ \text{(kJ/kg K)}\ (68.24 - 34.00)\ (^\circ\text{C})$$
$$= 118.8\ \text{kW}$$

The heat-transfer rate is calculated on the steam side of the heater using Eq. (9) from the measurements of the condensate flowrate, the supply pressure of the saturated steam and the temperature of the saturated liquid condensate. The enthalpy of the saturated vapor supply steam at 336 kPa is found in the steam tables (2730 kJ/kg), as is the enthalpy of the saturated liquid condensate at 192 kPa and 119 °C (499 kJ/kg). The heat transferred from the condensing steam is found using

$$Q_S = F_S \left(H_{supply} - H_{condensate}\right) \tag{9}$$

$$Q_S = 0.0482\,\text{(kg/s)}\left[2,730\,\text{(kJ/kg)} - 499\ \text{(kJ/kg)}\right]$$
$$= 107.5\,\text{kW}$$

Note that these two heat-transfer rates do not match perfectly.

2. Cooler:

The heat-transfer rate is calculated on the process-water side of the cooler using Eq. (10) from the measurements of the process-water flowrate and its inlet and outlet temperatures.

$$Q_{PWC} = F_{PW} c_p \left(T_{PWC,in} - T_{PWC,out}\right) \tag{10}$$

$$Q_{PWC} = 0.8275\ \text{(kg/s)}\ \ 4.194\ \ \text{(kJ/kg-K)}\ \ (68.24 - 33.26)(^\circ\text{C})$$
$$= 121.4\ \text{kW}$$

Of course, $T_{PWC,in}$ is equal to $T_{PWH,out}$.

The heat-transfer rate is also calculated on the cooling-water side of the cooler using Eq. (11) from the measurements of the cooling-water flowrate and its inlet and outlet temperatures.

$$Q_{CW} = F_{CW} c_p \left(T_{CW,out} - T_{CW,in}\right) \tag{11}$$

$$Q_{CWC} = 1.1\ \text{(kg/s)}\ \ 4.193\ \ \text{(kJ/kg-K)}\ \ (31.11 - 7.22)(^\circ\text{C})$$
$$= 110.2\ \text{kW}$$

The four heat duties are not exactly equal, which is an important lesson for the students to learn and will always be the case using experimental data. The maximum difference of 11.2 kW corresponds to a maximum error of 10%.

It should be noted that some data are more accurate than others. The process water and cooling water flowrate measurements are more reliable than the measurement of steam flowrate because there is some flashing of the condensate even when an ice bucket is used to capture the condensate leaving the steam trap.

Temperature differences between the inlet and outlet conditions are used in the heat duty calculations. The larger the temperature difference, the more reliable the calculations. For example, during experiment TP3 the process water is cooled 35.0 °C in the cooler, while the cooling water is heated only 23.9 °C.

As a result, among the four heat duties calculated above, the two process water heat duties are the most reliable and should be used in any other calculations for the experiment.

B. Calculation of Overall Heat-Transfer Coefficients

1. Heater:

Since the steam condenses at a constant temperature, the temperature driving forces at the ends of the heater are

$$\left(\Delta T_H\right)_2 = T_S - T_{PWH,in} = 118.9 - 34.0 = 84.9\ \text{K}$$
$$\left(\Delta T_H\right)_1 = T_S - T_{PWH,out} = 118.9 - 68.2 = 50.7\ \text{K} \tag{12}$$

where T_S is the saturation temperature of the steam at the pressure in the shell of the heater. The log-mean temperature driving force is then (see Figure 3):

$$\left(\Delta T_H\right)_{LM} = \frac{\left(\Delta T_H\right)_1 - \left(\Delta T_H\right)_2}{\ln\left(\dfrac{\left(\Delta T_H\right)_1}{\left(\Delta T_H\right)_2}\right)} = 66.3\ \text{K} \tag{13}$$

The overall heat-transfer coefficient is

$$U_H = \frac{Q_{PWH}}{A_H \left(\Delta T_H\right)_{LM}} \tag{14}$$

$$U_H = \frac{118.83\ \text{(kW)}}{05421\ \text{(m}^2\text{)}\ 66.3\ \text{(K)}} = 3,306\ \ \text{W/K} - \text{m}^2$$

There is no multiple-pass correction factor because the steam-side temperature is constant.

2. Cooler:

Similar calculations are carried out for the cooler. See Figure 3.

$$\left(\Delta T_C\right)_1 = T_{PWH,out} - T_{CW,in} = 68.2 - 31.1 = 37.1 \text{ K}$$
$$\left(\Delta T_C\right)_2 = T_{PWC,out} - T_{CW,out} = 33.3 - 7.2 = 26.1 \text{ K} \qquad (15)$$

$$\left(\Delta T_C\right)_{LM} = \frac{\left(\Delta T_C\right)_1 - \left(\Delta T_C\right)_2}{\ln\left(\frac{\left(\Delta T_C\right)_1}{\left(\Delta T_C\right)_2}\right)} = 31.3 \text{ K} \qquad (16)$$

$$U_C = \frac{Q_C}{A_C\left(\Delta T_C\right)_{LM} F_{corr}}$$
$$= \frac{121.4 \text{ (kW)}}{\left(2.957 \text{ m}^2\right)\left(31.3^\circ\text{K}\right)\left(0.96\right)} = 1{,}368 \text{ kW/K} - \text{m}^2 \qquad (17)$$

The 1-shell pass/4-tube pass correction factor F_{corr} = 0.96 is obtained from Fig.13.18a of Cengel.[3]

C. Velocities and Reynolds Numbers

The inside diameter of the tubes in the heater is 0.00475 m, and there are 54 tubes per pass. The velocity is

$$A_{CS,H} = 54\left(\pi D^2/4\right) = 0.0009569 \text{ m}^2$$
$$v_H = \frac{0.8275 \text{ (kg/s)}}{0.0009569 \text{ (m}^2\text{) } 987(\text{kg/m}^3)} = 0.877 \text{ m/sec} \qquad (18)$$

The Reynolds number is

$$(\text{Re})_H = \frac{D_H v_H \rho}{\mu} = \frac{0.00475 \text{ (m) } 0.877(\text{m/s}) \text{ } 987 \text{ (kg/m}^3)}{0.000552 \text{ (kg/m-s)}} = 7{,}444 \qquad (19)$$

The inside diameter of the tubes in the cooler is 0.00775 m, and there are 26 tubes per pass. The velocity is

$$A_{CS,C} = 26(\pi D^2/4) = 0.00123 \text{ m}^2$$
$$v_C = \frac{0.8275 \text{ (kg/s)}}{0.00123 \text{ (m}^2\text{) } 987 \text{ (kg/m}^3\text{)}} = 0.684 \text{ m/s} \qquad (20)$$

The Reynolds number is

$$(\text{Re})_C = \frac{D_C v_C \rho}{\mu} = \frac{0.00775 \text{ (m) } 0.684(\text{m/s}) \text{ } 987 \text{ (kg/m}^3\text{)}}{0.000555 \text{ (kg/m-s)}} = 9{,}418 \qquad (21)$$

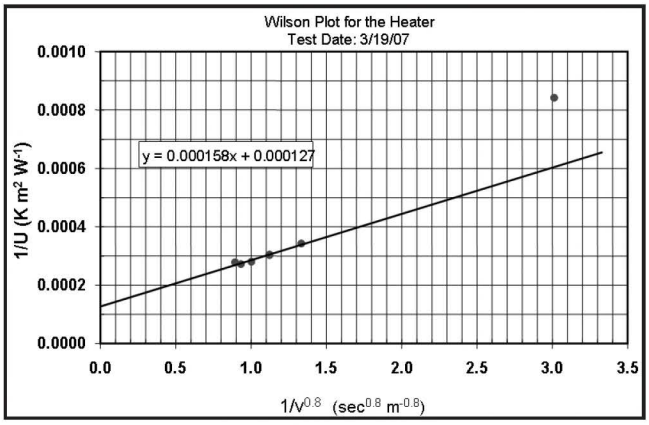

Figure 4.

WILSON PLOT FOR HEATER

A. Inside Film Coefficients:

Experimental data for a range of process-water flowrates are evaluated in a similar fashion as described above to calculate the overall heat-transfer coefficients and fluid velocities inside the tubes of the heater as well as the cooler. Results for critical parameters are presented in Table 3.

Since all but one data point have Reynolds numbers much greater than 2100, these data points are in the turbulent regime. Therefore, the constant "m" for the power of Re is assumed to be 0.8 according to the Dittus-Boelter correlation. For heating the fluid, again Dittus-Boelter suggests n=0.4 for the power coefficient of the Pr.

With these coefficients in mind, the Wilson plot for the heater data is shown in Figure 4. Several observations can be made from the Wilson plot.

- *The five data points with high Re show a linear trend. This confirms that the power of Re is equal to 0.8, as was assumed when constructing the Wilson plot.*
- *The point with the low Re (1865) shows*

TABLE 3. Operating Parameters for the Heater

m_{PW}	Avg. Temp.	Q_{PW}	Prandtl	Velocity	Re	U
(kg/s)	(°C)	(kW)	—	(m/s)	—	(W m^{-2} K^{-1})
0.241	42.5	38.9	4.20	0.252	1860	969
0.667	54.4	102.0	3.36	0.70	6330	2920
0.8275	51.1	118.8	3.56	0.877	7440	3300
0.953	50.8	134.6	3.58	1.009	8530	3570
1.044	50.3	137.6	3.62	1.105	9260	3670
1.099	50.3	134.8	3.62	1.164	9750	3590

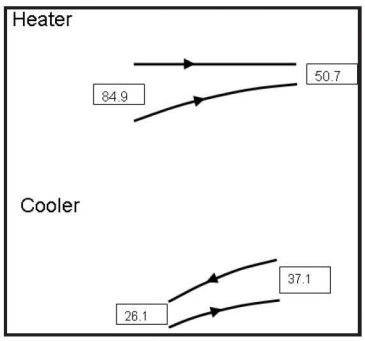

Figure 3.

a lower overall heat transfer coefficient as expected.

- *The regression line for the data points in the turbulent regime intersects the ordinate at $1/U_i = 0.000127$. Since the ordinate is where the process water velocity is infinite (infinitely large heat transfer coefficient inside the tube), this value is equal to coefficient "A" of Eq. (3a). Assuming minimal level of fouling inside and outside of the tube ($R_{fi} = R_{f0} = 0.00003$ m² K W⁻¹), the shell side film coefficient is calculated from Eq. (3a) to be 23,000 W m⁻² K⁻¹.*
- *The slope of the regression line is equal to the coefficient "B" in Eq. (7), which is used to calculate coefficient "C" in Eq. (4), as C = 0.020. The final correlation for the present experimental data is then:*

$$\mathrm{Nu} = \frac{h_i D_i}{k} = 0.020\ \mathrm{Re}^{0.8}\ \mathrm{Pr}^{0.4} \qquad (22)$$

Figures 5 and 6 compare experimentally found internal heat-transfer film coefficients to predictions by the Dittus-Boelter correlation. Figure 5 shows this comparison in a Nu/Pr^n vs. Re plot, and Figure 6 compares heat-transfer film coefficients. As indicated in Eq. (22), experimental results are 15% less than the predictions of the Dittus-Boelter correlation.

B. Repeatability:

The results of Wilson plot method are quite sensitive to the experimental uncertainty. This is illustrated in Figure 7, which shows two Wilson plots from the same facility but using data recorded on two different days. The circles are the data presented in Figure 4. The triangles represent results of the other experimental set of runs. It is seen that the two data sets provide two lines with different slopes. The slopes of the two data sets are 0.000158 and 0.0002, a difference of 25 %. This difference will of course affect the film coefficients similarly. This illustrates one of the problems with the Wilson plot method. The long extrapolation of the data points to zero on the abscissa makes the value of the intercept on the ordinate quite sensitive to the accuracy of the data.

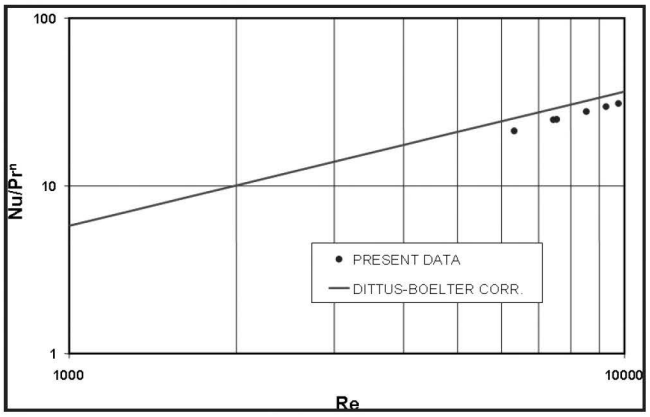

Figure 5.

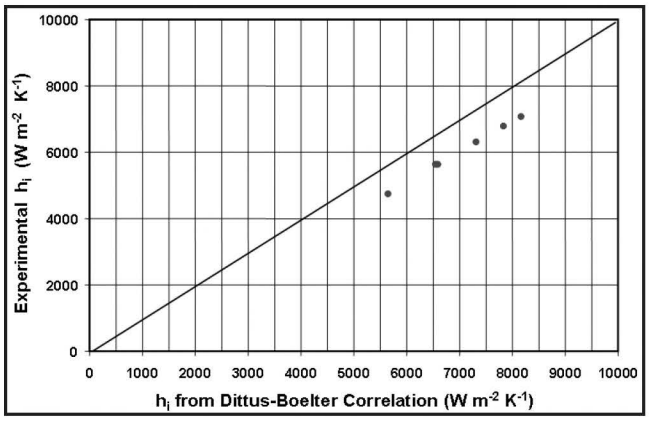

Figure 6.

DYNAMICS AND CONTROL

The steady-state experiments described above are performed by manually positioning the three control valves. In the control part of the experiment, two experimental identification techniques are used to find important dynamic features of the process: step testing and relay-feedback testing. Transfer functions and frequency response plots are generated from the experimental dynamic data. PI controllers are designed, and their closedloop performances are evaluated experimentally and compared with computer simulations of the dynamic process.

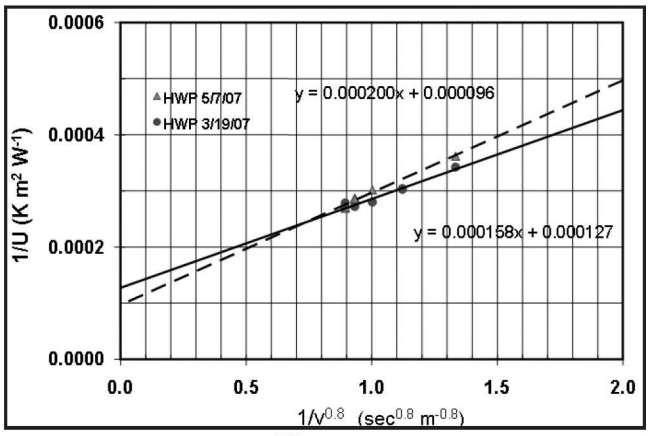

Figure 7.

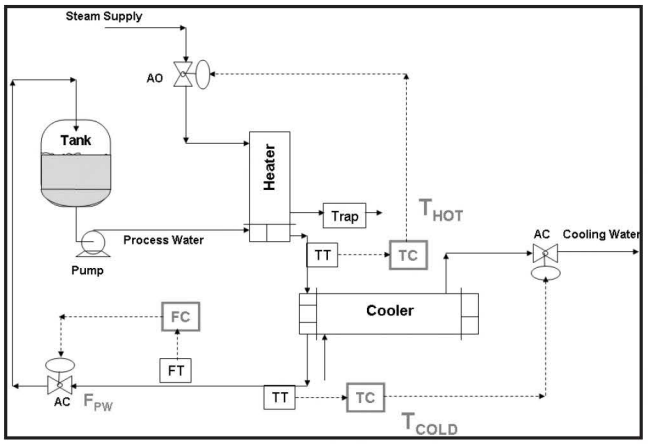

Figure 8.

One of the interesting control features of this experiment is dependence of the dynamics on the flowrate of the process water through the system. The higher the flow, the faster the dynamic responses of both heat exchangers. Controller tuning then depends on the process water flowrate.

A. Equipment and Control Structure:

Temperature and flowrate measurements are fed into a computer using A/D converters. LabView software has been developed that permits PI control with the three control valves positioned by three D/A converters from the computer. The steam valve is air-to-open, AO, so it will fail closed. The cooling water and process water valves are air-to-close, AC, so they will fail wide open.

The control structure is shown in Figure 8. There are three control loops.

1. *Process-water flowrate is controlled by manipulating the process-water control valve.*
2. *The process temperature leaving the heater, T_{HOT}, is controlled by manipulating the steam valve.*
3. *The process temperature leaving the cooler, T_{COLD}, is controlled by manipulating the cooling water valve.*

A screen shot is given in Figure 9 showing the three controller faceplates on the left. Each has a manual/automatic switch and displays for the setpoint (SP), the process variable (PV) and the controller output (OP).

B. Flow Control of Process Water:

The standard tuning of a flow controller is $K_C = 0.5$ and $\tau_I = 0.3$ minutes. The loop is quite fast since the flow transmitter and the valve respond quickly. Therefore a small integral time can be used. The gain is kept small so that the noise of the flow transmitter is not amplified.

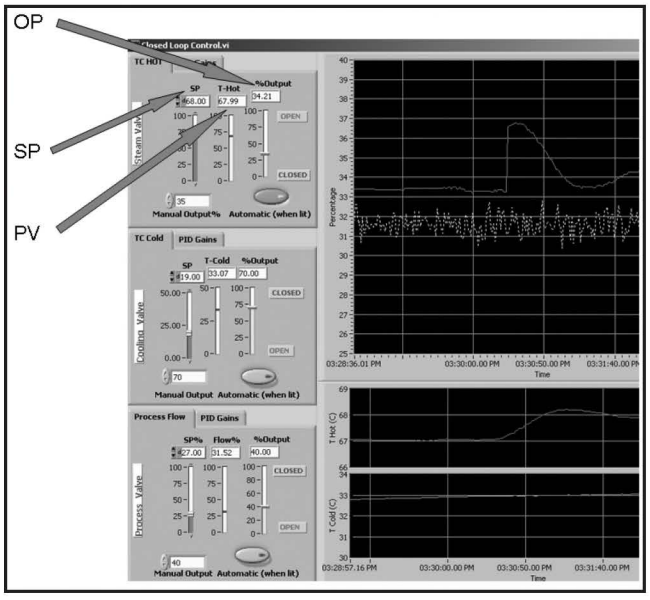

Figure 9.

The process water valve is AC, so the flow controller should have *"direct"* action (an increase in the flow transmitter signal PV produces an increase in the controller output signal OP to the valve, which reduces the opening of the valve). The equation of a PI controller is:

$$OP = Bias \pm K_C\left(E + \frac{1}{\tau_1}\int E\,dt\right)$$
$$E = SP - PV \qquad (23)$$

A direct-acting controller should have a negative gain. Step changes in the setpoint of the flow controller are made to confirm that the tuning constants used give good flow control performance.

C. Step Tests:

With both temperature controllers on manual, positive and negative step changes in the heater exit temperature controller output signal to the steam valve are made to identify a transfer function relating the controller OP signal to process PV signal (T_{hot}). See Figure 10.

From the dynamic step response, an approximate transfer function of the form given in Eq. (24) is determined.

$$G_{M(s)} = \frac{PV_{(s)}}{OP_{(s)}} = \frac{K_p e^{-Ds}}{\tau_o s + 1} \qquad (24)$$

where K_p is the process steady-state openloop gain, D is the deadtime and τ_o is the openloop time constant. The process gain K_p must be dimensionless, so the change in temperature must be divided by the temperature transmitter span (100 °C) to convert the PV signal to percent of scale. The OP signal is in percent of scale. The experimental data in Figure 10 show a deadtime of 0.2 minutes, a time constant of 1.1 minutes and a gain of 0.7.

The ultimate gain K_u and ultimate frequency ω_u are calculated from the transfer function using the relationships at the

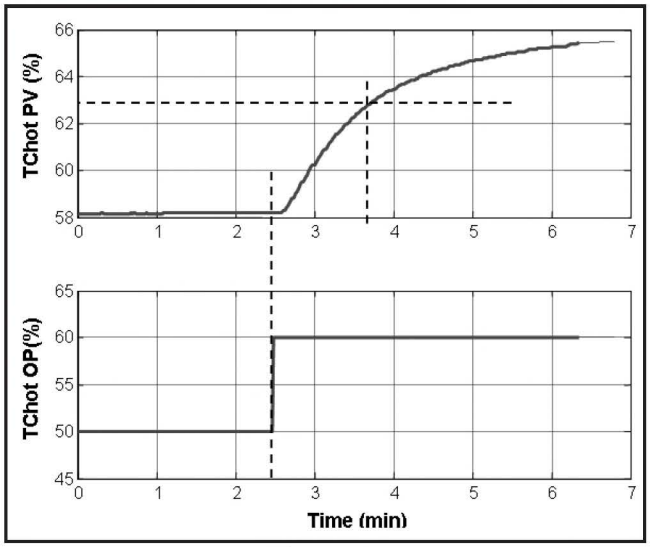

Figure 10.

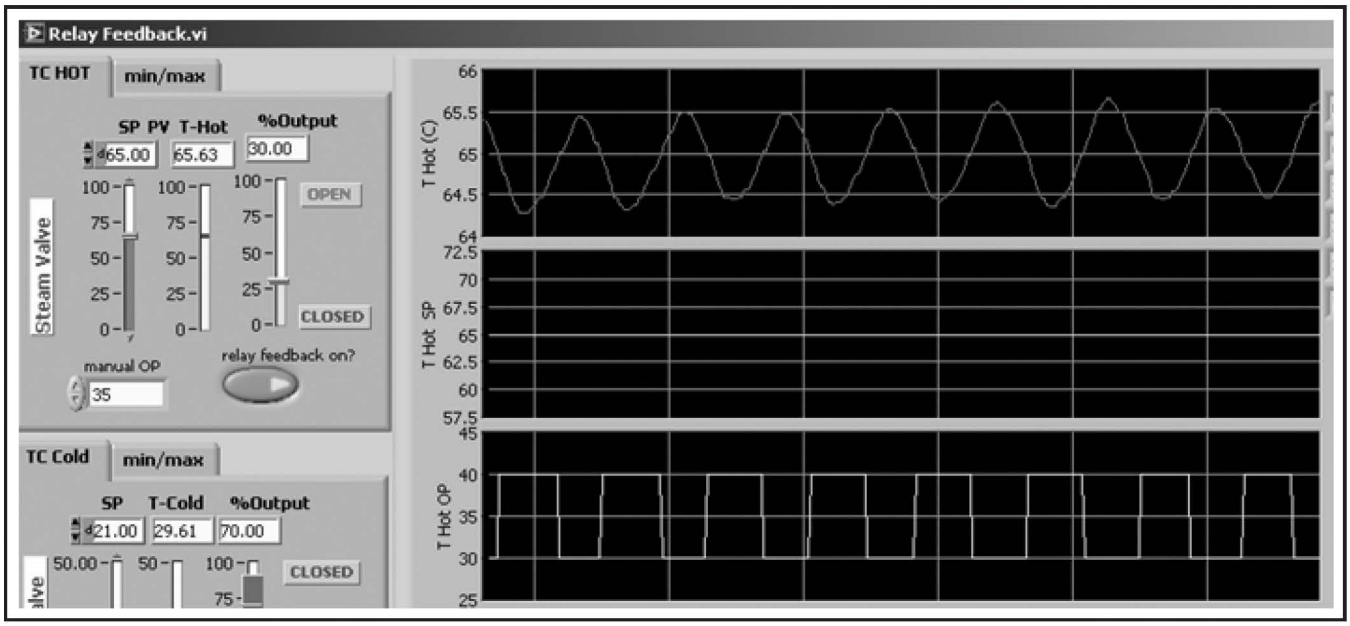

Figure 11.

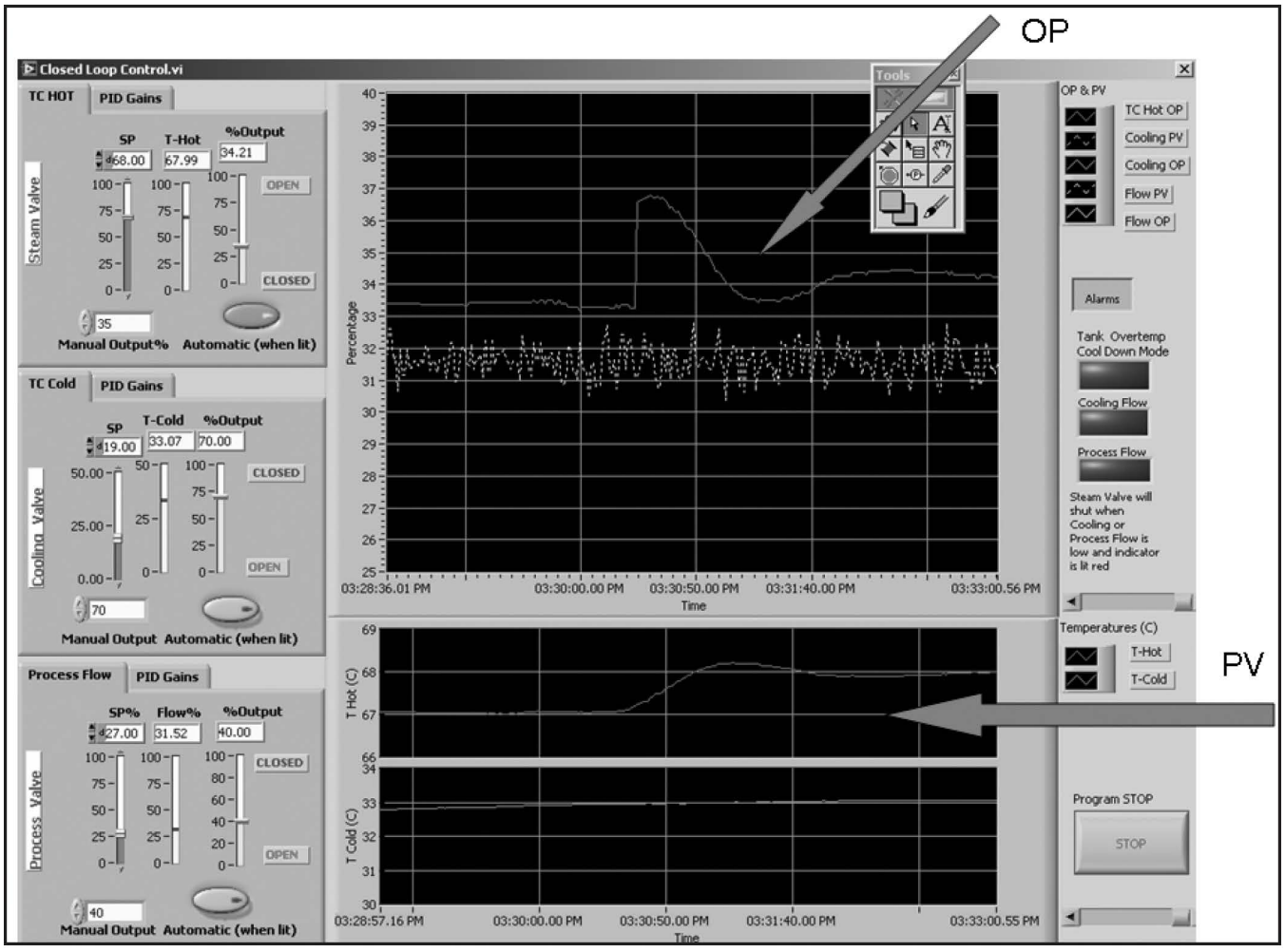

Figure 12.

ultimate frequency ω_u.

$\arg G_M(i\omega_u) = D\omega_u - \arctan(\omega_u \tau_o) = -\pi$ radians.

$$\left|G_{M(i\omega_u)}\right| = \frac{K_p}{\sqrt{1+\left(\omega_u \tau_o\right)^2}} = \frac{1}{K_u} \qquad (25)$$

The step test results predict an ultimate frequency of 8.4 radians/minute and an ultimate gain of 13.

D. Relay-Feedback Test

The relay-feedback test is a very simple, fast, and practical method for determining accurate information for tuning of feedback controllers. It is widely used in industry and is also included in commercial dynamic simulators to facilitate controller tuning. The test gives values for the ultimate gain and period.

A high-gain relay is inserted in the feedback loop that switches the controller output signal a specified "h" percent above or below the steady-state OP value as the PV signal crosses the SP setpoint signal. The SP signal is adjusted so that the signal to the control valve varies between the ± h limits in *symmetrical* pulses (approximately the same time at the low limit as at the high limit). Figure 11 gives a screen shot of the monitor when the relay-feedback test is running.

The amplitude "a" of PV temperature sinusoidal signal T_{hot} and the period P_u are read from a strip chart. The amplitude a must be in % of scale, using a temperature transmitter span of 100 °C. Note that h is also in percent of scale.

The ultimate gain and ultimate frequency from the experimental curves are calculated and compared with the values obtained from the transfer function.

$$K_u = \frac{4h}{a\pi} \qquad (26)$$

Figure 11 shows a plot of typical data. The value of a is 0.6 % with a 5% h, and the period is 0.7 minutes. The calculated ultimate gain is 10 and the ultimate period is 0.7 minutes, giving an ultimate frequency of 9 radians/minute. These results are fairly close to those determined from the step test data and are more reliable because of the closedloop nature of the relay-feedback test, which keeps the process in the linear region.

E. Closedloop Control

The Tyreus-Luyben tuning constants are calculated, and their performance for disturbances in setpoints and process water flowrate are observed.

Tyreus-Luyben:

$$K_c = \frac{K_u}{3.2} = \frac{10}{3.2} = 3.1$$
$$\tau_I = 2.2\,P_u = 2.2(0.7) = 1.5\,\text{minutes} \qquad (27)$$

Figure 12 shows the closedloop step response of the T_{HOT} temperature controller for a change in setpoint using TL tuning. The setpoint is changed from 67 °C to 68 °C (a 1% of scale change). The OP signal jumps immediately from 33.3% to 36.4% from the proportional action (K_C = 3.1). There is a slight overshoot of the setpoint, and it takes about 3 minutes for the loop to settle out.

The closedloop response of the system for load disturbances is also explored by making changes in the flowrate of the process water. Process nonlinearity is studied by seeing how the dynamics of the process change at different process water circulation rates. Time constants decrease as process water flowrates increase.

COMPUTER SIMULATIONS

Our students use process simulation tools extensively in their design course to develop process flowsheets and study dynamic plantwide control. Applying these tools for the heat exchanger experiment provides an important exercise in comparing model predictions with real experimental data.

A. Steady-State Flowsheet Simulation:

A steady-state simulation of the two-heat exchanger and feed tank system is developed in Aspen Plus. Equipment sizes, operating conditions, and experimental heat-transfer parameters are used to match experimental steady-state conditions.

The *HeatX* unit is used in the *Short-cut* and *Design* modes. The inlet conditions of the steam and the process water are specified in the heater. In addition, the hot condensate stream leaving the heater is specified to have a vapor fraction of zero, as shown in Figure 13A. Figure 13B shows that the overall heat-transfer coefficient U is specified to be the experimen-

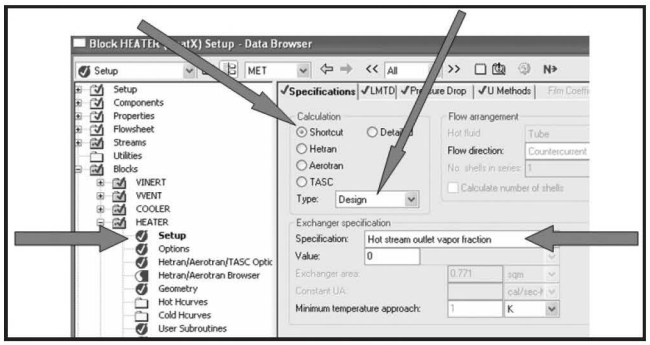

Figure 13A.

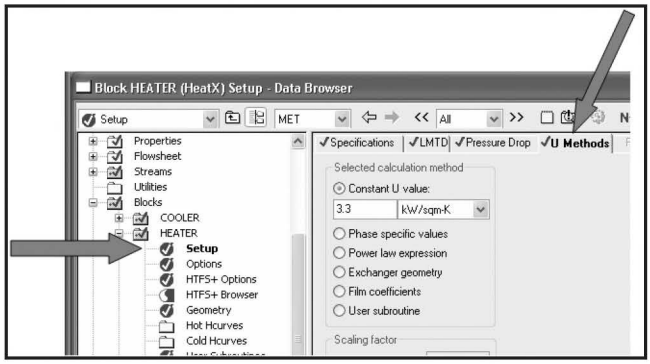

Figure 13B.

tal value (3.3 kW m^{-2} K^{-1}). The program then calculates the required area, which is almost exactly the real heat-transfer area of the heater.

The specification for the cooler, besides the inlet conditions of the cooling water and the process water, is the exit temperature of the process water, as shown in Figure 14.

The simulation is pressure driven, so pressures throughout the process must be specified. The pump discharge pressure is set at 5 atm in the simulation, and 1 atm pressure drops of the process water through each heat exchanger are assumed. The steam supply pressure is 3.3 atm with 1.5 atm in the shell side of the heater. The cooling water supply pressure is 5 atm, and the pressure drop through the cooler is assumed to be 1 atm. Since Aspen Plus does not permit the use of anything other than direct-acting control valve with linear trim, the steady-state positions of all control valves is set at 50% open in the simulation. Figure 15 gives the steady-state

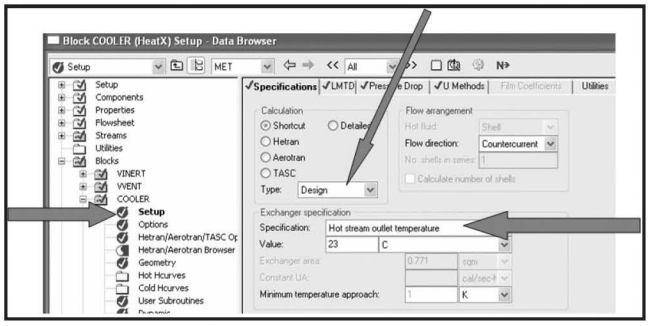

Figure 14.

	PWIN	PWOUTH	PWOUTC	STEAM	COND	CWIN	CWOUT
Temperature K	300.3	340.0	300.0	410.5	385.0	280.1	310.7
Pressure atm	5.00	4.00	3.00	3.30	1.50	5.00	4.00
Vapor Frac	0.000	0.000	0.000	1.000	0.000	0.000	0.000
Mole Flow kmol/hr	165.038	165.041	165.041	11.506	11.506	225.808	225.808
Mass Flow kg/hr	2974.355	2974.414	2974.414	207.288	207.288	4068.000	4068.000
Volume Flow l/min	50.023	52.087	50.008	1957.387	3.816	67.082	69.088
Enthalpy MMBtu/hr	-44.633	-44.186	-44.638	-2.596	-3.044	-61.407	-60.955
Mass Flow kg/hr							
WATER	2971.114	2971.173	2971.173	207.288	207.288	4068.000	4068.000
N2	3.242	3.242	3.242				
Mole Flow kmol/hr							
WATER	164.922	164.925	164.925	11.506	11.506	225.808	225.808
N2	0.116	0.116	0.116				

Figure 15.

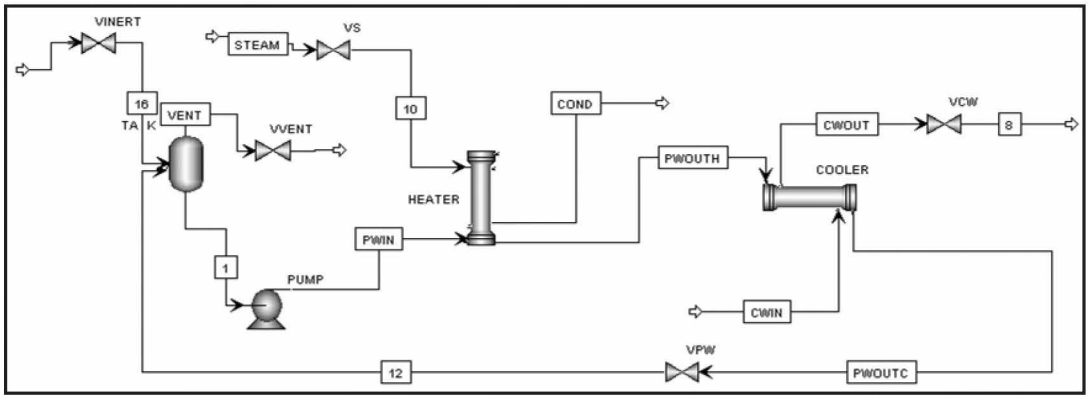

Figure 16.

stream information. The Aspen Plus process flow diagram is shown in Figure 16.

Note that a small nitrogen stream is fed into the feed tank and a vapor stream is removed. This is a simulation gimmick to account for the tank being open to the atmosphere.

B. Dynamics Simulation:

Before dynamics can be simulated, the volumes and weight of metal in the various units must be specified. These are calculated from the dimensions of the tubes and shell. Figure 17 shows how these are specified in the simulation by selecting the *Dynamic* item in the heater block. The file is pressure checked and exported into Aspen Dynamics as a pressure-driven simulation.

Figure 18 shows the initial process flow diagram generated in Aspen Dynamics. Controllers are installed by opening *Libraries*, *Dynamic*, and *ControlModels* in the *Exploring-Simulation* mode on the left side of the screen. A controller is inserted on the flowsheet by clicking on *PIDIncr* and dragging and dropping. Deadtimes are inserted in the same way.

The controllers are connected to the appropriate streams and valves by opening *Stream Types*, dragging a *ControlSignal* to the flowsheet and connecting its two ends to the appropriate spots. Figure 19 shows the TChot controller. It measures the temperature of the process water leaving the heater. The signal goes through a first-order lag and a deadtime before becoming the PV signal of the TChot temperature controller. The controller output positions the steam valve.

Figure 20 shows the controller faceplate. The third button from the right is clicked to open the window shown below the faceplate. The controller action is set to be *Reverse* since an increase in temperature should lower the OP signal. The deadtime in this loop is set at 0.1 minutes, and the lag time constant is set at 0.4 minutes. These values give an ultimate gain and frequency that match fairly closely the experimental values.

One of the unique features of the heater is the requirement that the condensate leaving must be saturated liquid (a vapor fraction of zero). In Aspen Dynamics, this condition is not the default. Instead the pressure is fixed. Of course, this is not what really happens. To increase flow of steam to the heater, the steam valve opens and the pressure on the steam side of the heater must increase to provide a higher temperature differential driving force. Therefore, some modifications must be made to simulate reality.

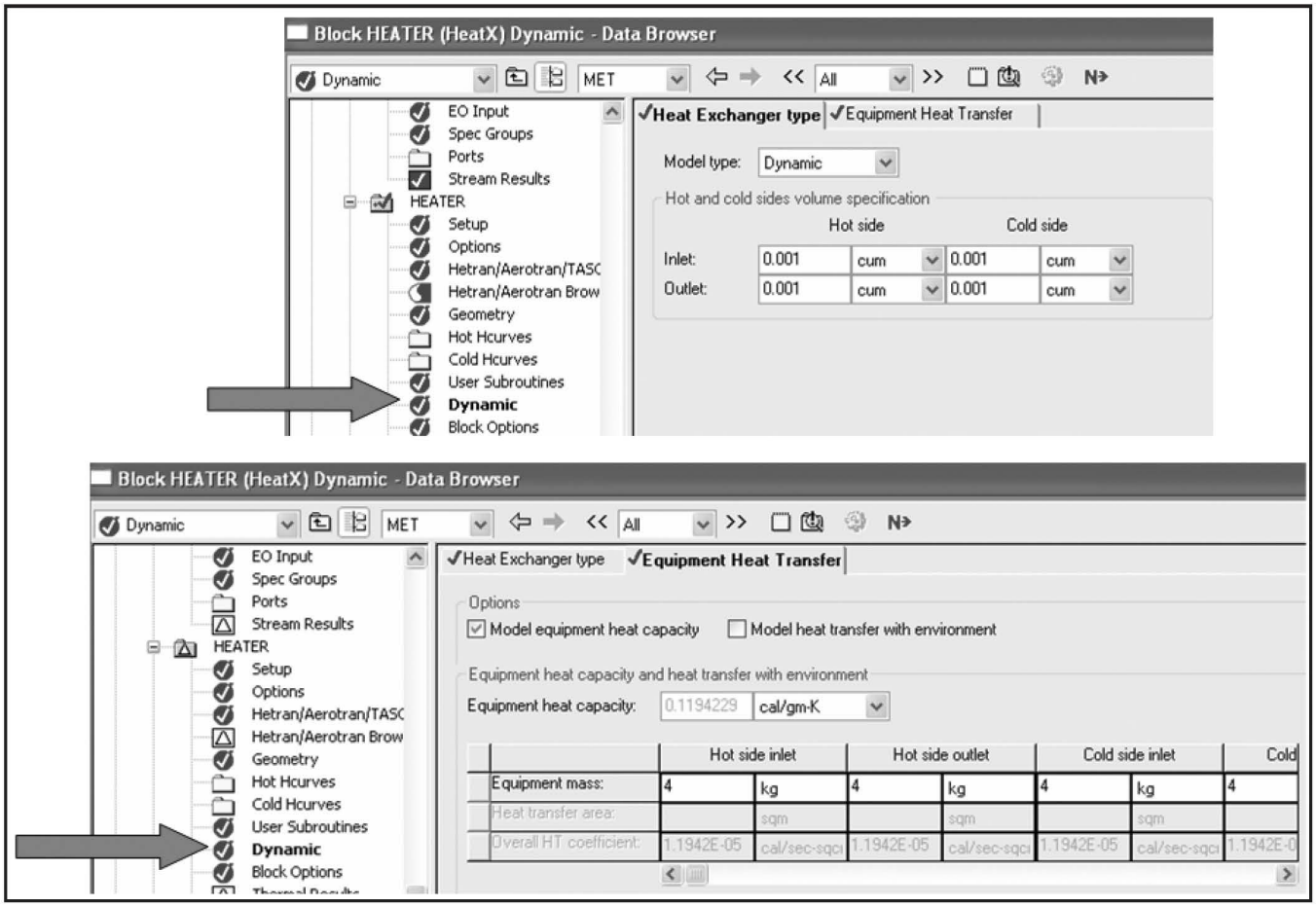

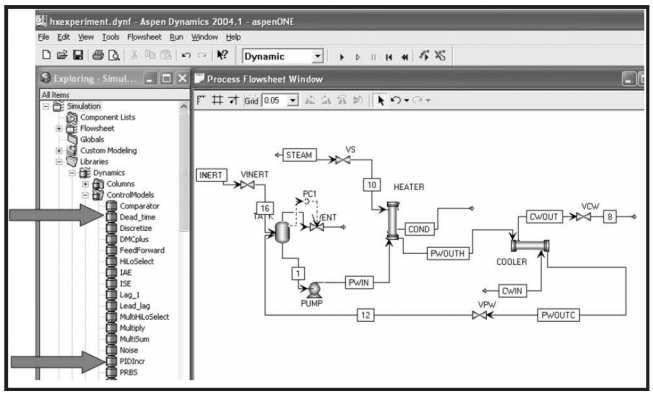

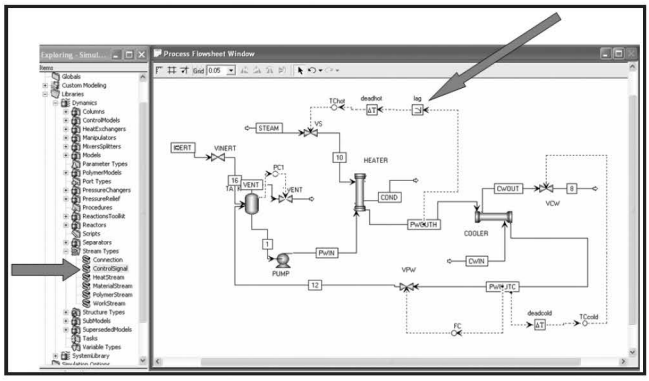

▲ *Top:* ***Figure 17.***

◀ *Left:* ***Figure 18.***

▶ *Bottom left:* ***Figure 19.***

▼ *Bottom right:* ***Figure 20.***

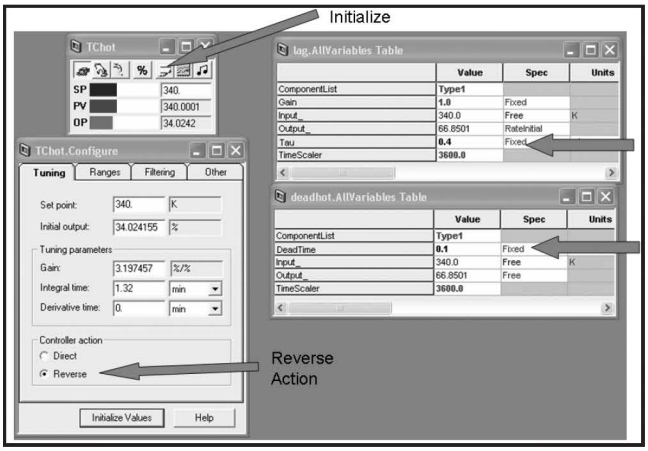

► *Right:* ***Figure 21.***

▼ *Below:* ***Figure 22.***

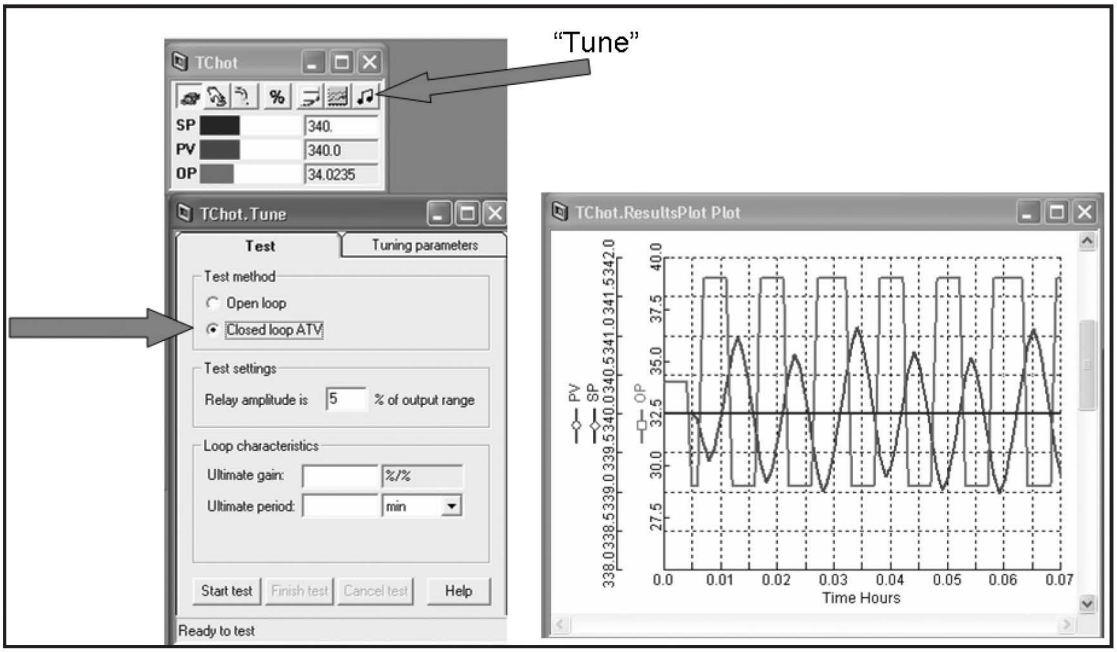

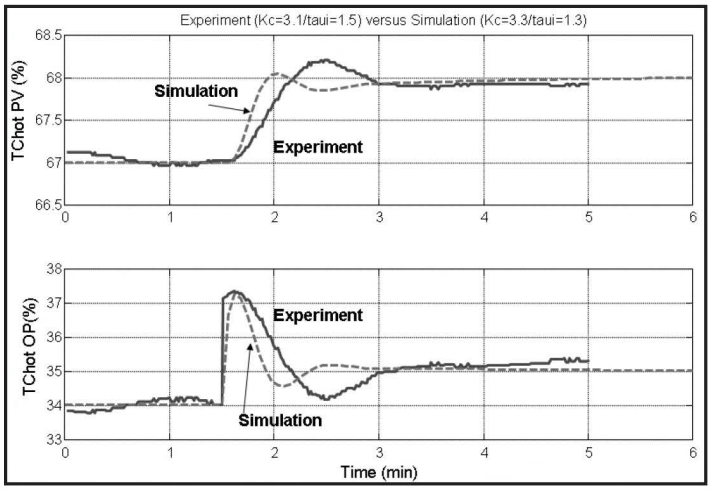

These are achieved by using *Flowsheet Equations*. The heater block is specified to have a hot stream leaving with a vapor fraction of zero.

Blocks("Heater").Hotside.pflash2(1).vfr=0;

In addition, the pressure of the condensate stream "COND" is changed from "fixed" to "free."

C. Dynamic Results:

Step changes are made by putting the controller on manual and changing the OP signal. Relay-feedback tests are run by clicking the *Tune* button on the controller faceplate (see Figure 21). The Closed loop ATV test is selected. The simulation is run until a steady state is obtained with the controller on automatic. Then the *Start test* button is clicked, and the process is allowed to run through several cycles, as shown in the strip chart in Figure 21. Clicking the *Finish test* button generated the ultimate gain and period: K_u = 10.2 and P_u = 0.60 minutes for the TChot controller.

Opening the *Tuning parameters* page tab, selecting the type of controller and the tuning rule and clicking the *Calculate* button produce the controller tuning constants. These settings are inserted into the controller by clicking the *Update controller* button.

Figure 22 gives a direct comparison between the experimental and simulation responses for a step change in setpoint of 1 K. The dynamics of the heater are fairly well predicted by the Aspen Dynamics simulation.

CONCLUSION

This paper has described an experiment that combines steady-state heat transfer analysis and dynamic controllability. The heat transfer analysis includes data reconciliation of redundant and conflicting temperature measurements by checking energy balances on both sides of the two heat exchangers. The Wilson plot method is used to calculate tube side film coefficients from the measured overall heat transfer coefficients.

Experimental dynamic data is obtained from step and relay-feedback tests. Both steady-state conditions and control performance are compared with the predictions of a commercial process simulator.

REFERENCES

1. Wilson, E.E., "A basis for rational design of heat transfer apparatus," *Trans. Am. Mech. Engrs.*, **37**, 47 (1915)
2. Hewitt, G.F., Shires, G.L. and Polezhaev, Y.V., *International Encyclopedia of Heat & Mass Transfer*, CRC Press, New York (1997)
3. Cengel, Y.A., *Heat Transfer*, McGraw Hill, New York, (2003) ❐